Three-Dimensional Finite Element Analysis and Experiment of Temperature Rise of Permanent Magnet Linear Synchronous Motor

Jianjian Fan and Mengjie Shen

Abstract Permanent magnet linear synchronous motors (PMLSM) are widely used in semiconductor processing, laser cutting, inspection and precision positioning because of high thrust density, high power density, high acceleration, fast response, good reliability and high precision. The torque of the PMLSM is proportional to the input current, that is, to output large electromagnetic thrust, the PMLSM needs a large input current. The large current will cause large losses, mainly copper loss in the winding, which will eventually heat up the winding and other parts and cause temperature rise. High temperature rise will reduce the motor's insulation life or even destroy the insulation, which will reduce the performance of the motor or cause the motor failure. Thus, by studying and analyzing the temperature rise of PMLSM, it is beneficial to achieve rational design or motor operating condition prediction. In this paper, finite element modeling analysis of the three-dimensional temperature field of the motor is conducted based on a linear motor test rig, which includes a linear motor, a sliding table, a linear bearing, a linear module base and a marble platform. The finite element analysis results are compared with the experiment results and they are consistent. This paper provides a reference method for linear motor temperature rise analysis.

Keywords Permanent magnet linear synchronous motor · Temperature field · Finite element · Fluent · Temperature rise experiment

J. Fan (✉)
Zhejiang University of Water Resources and Electric Power, Hangzhou, China
e-mail: 26616742@qq.com

M. Shen
Zhejiang Hiatran Electric Technology Co., Ltd, Hangzhou, China
e-mail: shenmengjie@hiatran.com

G. L. Conte and O. Sename (eds.), *Proceedings of the 11th International Conference on Mechatronics and Control Engineering*, Lecture Notes in Mechanical Engineering,
https://doi.org/10.1007/978-981-99-6523-6_1

1 Introduction

Permanent magnet linear synchronous motors (PMLSM) are widely used in semiconductor processing, laser cutting, inspection and precision positioning because of high thrust density, high power density, high acceleration, fast response, good reliability and high precision [1, 2]. The torque of the PMLSM is proportional to the input current, that is, to output large electromagnetic thrust, the PMLSM needs a large input current. The large current will cause large losses, mainly copper loss in the winding, which will eventually heat up the winding and other parts and cause temperature rise. High temperature rise will reduce the motor's insulation life or even destroy the insulation, which will reduce the performance of the motor or cause the motor failure. Thus, by studying and analyzing the temperature rise of PMLSM, it is beneficial to achieve rational design or motor operating condition prediction. However, the influence of the linear module base and test platform of the linear bearing on the temperature rise of the motor has not been taken into account yet.

Due to the special structure and special operating conditions (such as round-trip, transient high thrust, intermittent operating mode and etc.) of linear motors, the thermal analysis of liner motors by thermal resistance-network analysis (TRA) and finite-element analysis (FEA) are significantly different than those conventional rotating motors, as a result, the study of linear motor temperature fields are few. However, as the linear motors are more and more widely used, the related temperature field analysis has been increasingly attention.

A detailed analysis of the temperature field of a water-cooled large-thrust permanent magnet synchronous motors was carried out by FEA, TRA and experiments in [1], and the simulation result and calculated values were consistent with the experiment results. However, this study only performed a two-dimensional analysis, and the analysis report was only the motor itself. In [3], the three-dimensional temperature field of an asynchronous starting permanent magnet motor has been studied. The analysis uses fluent, a FEA software, to model the temperature field and considers the rotor rotation through the equivalent air gap length, while also considering the effect of bearing thermal conduction on the temperature rise.

The temperature rise of a linear motor was investigated by TRA [4], and compared with experiment results the method is proved to be feasible, but TRA requires a lot tedious equivalent calculations for each part of the motor thermal circuit. In [5], the temperature field analysis of a PMLSM which mounted on a movable substrate base plate operating at low speed was carried out by FEA.

In this paper, finite element modeling analysis of the three-dimensional temperature field of the motor is conducted based on a linear motor test rig, which includes a linear motor, a sliding table, a linear bearing, a linear module base and a marble platform. The three-dimensional finite element temperature field model of the motor is firstly established, the losses of the motor were analyzed and the boundary conditions of the temperature field are determined to solve the temperature field. Secondly, temperature rise experiments were conducted based on the prototype. Finally, the

simulation and experiment results are compared and they are consistent. This paper provides a reference for the linear motor temperature rise analysis.

2 Motor Temperature Model

The linear motor test system, as shown in Fig. 1, consists of a marble platform, a linear module base, the stator and mover of the PMLSM, the test bench, a connecting device for test and a load liner motor. PMLSM is a single-sided flat type with iron core structure, the stator consists of back iron, permanent magnets, and permanent magnets stainless steel sheath; the mover consists of winding, iron core, slot insulation and epoxy resin. The motor parameters are shown in Table 1. The motor is naturally cooled and the operating speed is 0.2 m/s.

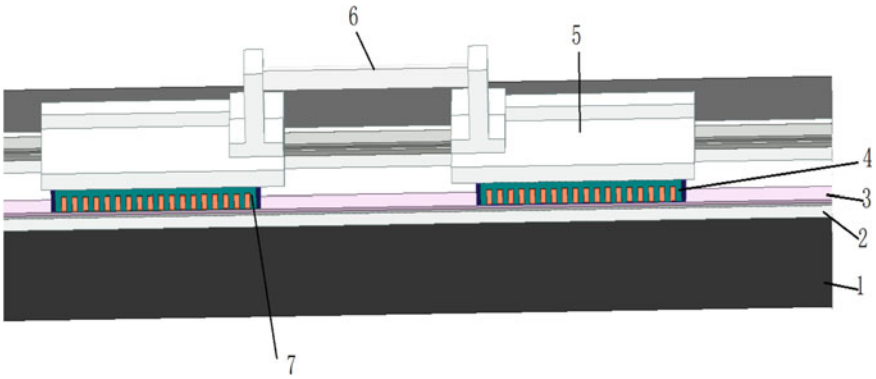

Fig. 1 Temperature rise test platform for PMLSM. 1-Marble platform, 2-Linear module base (linear bearing, slider and guide rail), 3-Stator of linear motor (include back iron, permanent magnets, permanent magnets stainless steel sheath), 4-Mover of the Linear motor, 5-Sliding table, 6-Connecting device for test, 7-Load linear motor

Table 1 Parameters of PMLSM and test rig

Parameters	Value	Parameters	Value
Mover length (mm)	300	Sliding table length (mm)	360
Mover width (mm)	55	Sliding table width (mm)	200
Mover height (mm)	31	Sliding table height (mm)	23.4
Air-gap length (mm)	0.6	Current (A)	4.5
Stator height (mm)	8.4	Line resistance (25 °C) (Ω)	4.5
Module base length (mm)	2500	Marble platform width (mm)	400
Module base width (mm)	210	Marble platform thickness (mm)	130
Module base thickness (mm)	36		

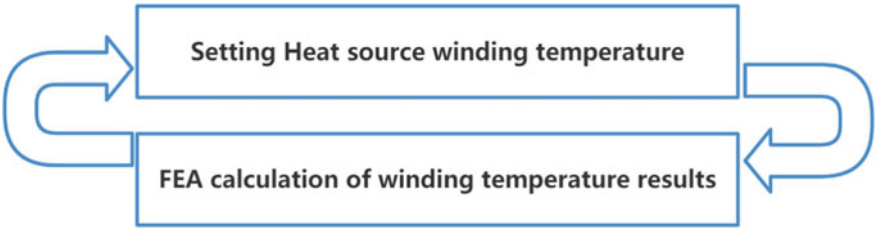

Fig. 2 Temperature iteration of PMLSM

Table 2 Losses of linear motor (25 °C)

Parameters	Value (W)	Percent (%)
Iron loss	0.55	0.39
Eddy current loss	0.01	0.01
Mechanical loss	3.08	2.19
Copper loss	136.68	97.41

2.1 Motor Loss

The losses of the PMLSM include copper loss, iron loss, mechanical loss, and eddy current loss. Due to the low motor operating speed of 0.2 m/s, the iron loss and eddy current loss can be neglected. The mechanical loss is mainly the linear bearing loss, which can also be ignored. The friction force of the sliding table is only 15.4 N as measured, so the heat generated by it can be ignored too. The main loss of the motor is the copper loss, $P_{cu} = 1.5*I^2*Rt$, I is the motor RMS current, Rt is the winding resistance at t°C. When the motor winding temperature is 25 °C, the winding resistance is 4.5 Ω, and winding copper loss is 137 W at the rated current. The winding copper loss at t°C can be expressed as $P_{cu} = 137*(235 + t)/(235 + 25)$, and the value of t can be determined by iterative temperature solution, and the iterative process is shown in Fig. 2. The loss value of each part of the motor (mechanical loss is determined by measurement) at 25 °C are shown in the following Table 2. Table 2 illustrates that the other losses in motor can be ignored, so only the copper losses are considered in the analysis.

2.2 Temperature Field Model

Given by thermodynamics and [6], In the Cartesian coordinate system, the three-dimensional transient heat conduction equation and its boundary condition is given by

$$\begin{aligned}
&\frac{\partial}{\partial x}\left(k_x\frac{\partial T}{\partial x}\right)+\frac{\partial}{\partial y}\left(k_y\frac{\partial T}{\partial y}\right)+\frac{\partial}{\partial z}(k_z)+q=\rho c\frac{\partial T}{\partial t}\\
&S_1: T=T_0\\
&S_2: k\frac{\partial T}{\partial t}=-q_0\\
&S_3: k\frac{\partial T}{\partial n}=-\mathrm{h}(T-T_e)
\end{aligned} \tag{1}$$

where T is the object temperature, T_0 is the known temperature distribution on the boundary; T_e is the temperature of the surrounding medium; k_x, k_y, k_z are the thermal conductivity of the object in the x, y, z direction, respectively; q is the density of the heat source; q_0 is the density of heat flow through the boundary surface S_2; n is the boundary normal vector; h is the heat transfer coefficient; k is the thermal conductivity; ρ is the density; c is the specific heat.

In order to improve the efficiency of the temperature field finite element model calculation, the following assumptions are made.

1. The copper losses are uniformly distributed by volume in the straight and end sections of the coil.
2. The mover is stationary during the analysis, and the air moves at 0.2m/s relative to the mover.
3. Marble platform temperature is 25 °C, ignore the contact thermal resistance between the linear module base and marble platform. Linear bearing using heat transfer coefficient instead of its actual ball thermal conductivity and lubricant convection heat dissipation, ignore the marble platform and module base.
4. Ignore the temperature conduction between the motor and the load motor. The temperature field model is established as a symmetric half model along the direction of motion.
5. Ignore the openings and chamfer on each component, do not consider the influence of lubrication and thermal radiation on heat transfer, convection heat transfer coefficient is a fixed value, only the copper loss varies with temperature to simplify the modeling and calculation.
6. Separation of copper and insulating varnish.

According to the assumptions and temperature field equations to establish a three-dimensional finite element analysis model of the linear motor as shown in Fig. 3.

The individual material properties in the model are shown in Table 3.

The key to the temperature field solution is to determine the heat transfer coefficient of each face, such as forced convection heat transfer coefficient of each face of the mover, and the natural heat transfer coefficient of each face of the stator. The difficulty in solving the temperature field is to determine the thermal conductivity of the bearing, which involves fluid convection and solid thermal conductivity. The analysis of the heat transfer coefficient involves the following common constants.

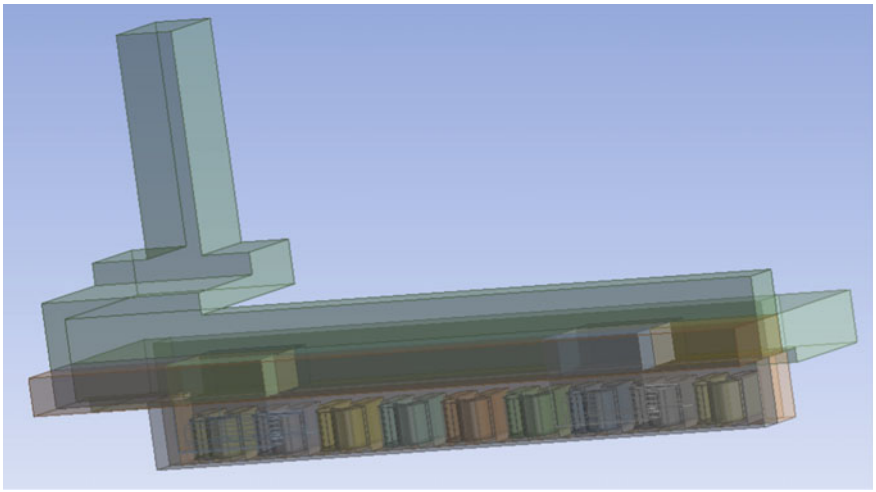

Fig. 3 Finite element analysis model of PMLSM

Table 3 Material thermal parameters

Materials	Density (kg/m^3)	Specific heat capacity (k/j)	Thermal conductivity (W/k.m)
Silicon steel sheet	7700	434	X: 39, Y: 4.43, Z: 39
Copper	8890	380	X: 385, Y: 1.5, X: 1.5
Epoxy resin	1800	900	0.8
Aluminum	2700	460	385
Air	1.205	1005	0.026
Slot insulation	930	1340	0.18

Reynolds number:

$$\mathrm{R_e} = \frac{\mathrm{u}l}{\upsilon} \tag{2}$$

Rayleigh number:

$$\mathrm{R_a} = G_r \cdot P_r \tag{3}$$

Grashof number:

$$G_r = \frac{gl^3\alpha\Delta t}{\upsilon^2} \tag{4}$$

Prandtl number:

$$P_r = \frac{\upsilon}{a} \tag{5}$$

Nusselt number:

$$N_u = \frac{hl}{\lambda} \tag{6}$$

For the convective heat transfer coefficient [7] on the air gap surface is calculated as

For laminar flow ($R_e <= 5 \times 10^5$):

$$N_u = 0.644 R_e^{1/2} P_r^{1/3} \tag{7}$$

For turbulent flow ($5 \times 10^5 <= Re <= 10^8$):

$$N_u = \left(0.037 R_e^{0.8} - 870\right) P_r^{1/3} \tag{8}$$

For the convective heat transfer coefficient [8] at the front and rear ends of the movers is calculated

$$N_u = 0.2 R_e^{2/3} \tag{9}$$

For the stator surface, the natural heat transfer coefficient [8] is calculated:

For the horizontal plane:

(a) Upper surface of hot plate or lower surface of cold plate

$$N_u = 0.54 R_a^{1/4} \quad (10^4 <= R_a <= 10^7) \tag{10}$$

$$N_u = 0.15 R_a^{1/3} \quad (10^7 <= R_a <= 10^{11}) \tag{11}$$

(b) The lower surface of the hot plate or the upper surface of the cold plate

$$N_u = 0.27 R_a^{1/4} \quad (10^5 <= R_a <= 10^{10}) \tag{12}$$

For vertical surfaces:

$$N_u = \left\{ 0.825 + \frac{0.387 R_a^{1/6}}{[1 + (0.492/P_r)^{9/16}]^{8/27}} \right\}^2 \tag{13}$$

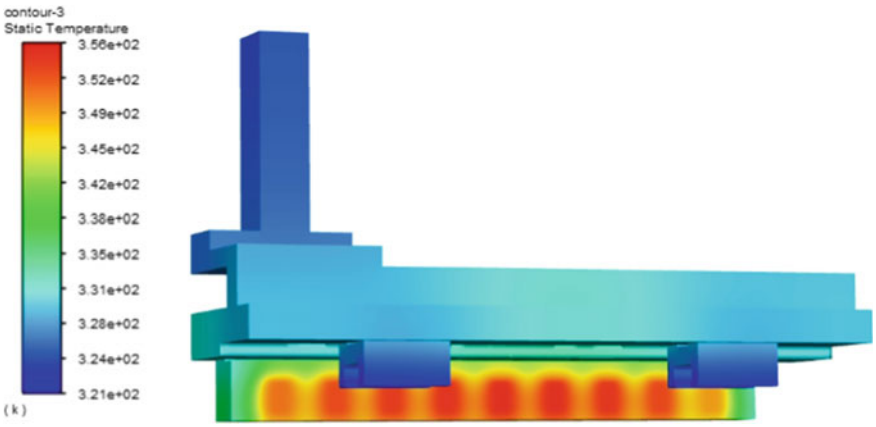

Fig. 4 Steady temperature cloud map of PMLSM

The simulation temperature of the core and winding of the motor is recorded and the temperature curve is shown in Fig. 7. The steady temperature cloud map of the PMLSM is shown in Fig. 4.

3 Experimental Validation

In order to verify the simulation result, the temperature rise test were conducted on the PMLSM as shown in Fig. 5. The temperature thermocouple probe was inserted into the stator core mounting hole and the average temperature rise of the winding was measured by the resistance method. During the test, the operating speed was 0.2 m/s and the distance was 1 m. The motor run in electric mode, while the load motor run in braking mode. The currents of the two motors during the operating cycle were 4.54 and 4.24 Arms. The current curves of the motor are shown in Fig. 5, and the oscilloscope showed a current value of 4.542 Arms during a round trip cycle. The temperature rise of the stator core which measured by the temperature probe is shown in Fig. 6. The line resistance and ambient temperature before and after the test is shown in Table 4.

4 Analysis and Discussion

The FEA results and temperature rise test data are summarized as shown in Table 5, Figs. 7 and 8.

As shown in Table 5, Figs. 7 and 8, it can be seen that the deviation between the finite element results and the measured results is small. The reason for the deviation

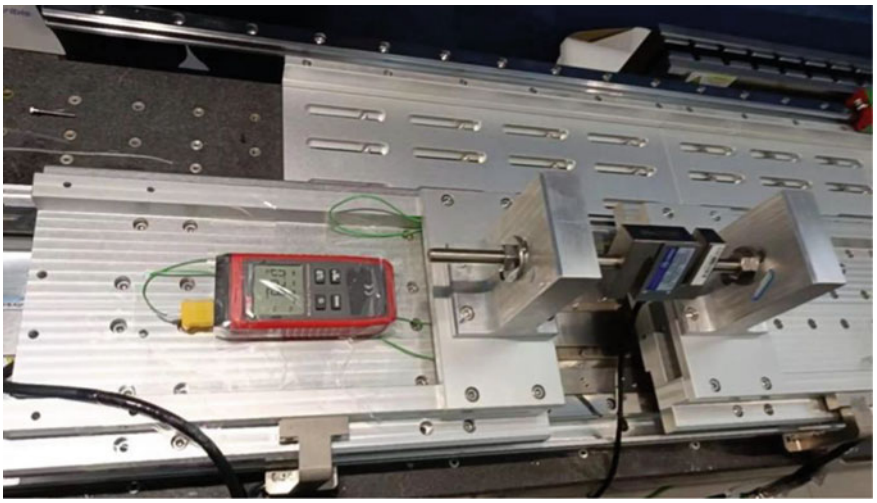

Fig. 5 Temperature rise test for PMLSM

Fig. 6 Current waveform

Table 4 PMLSM temperature rise test winding resistance and temperature

Parameters	Value	Unit
Ambient temperature	25	°C
Line resistance at ambient temperature	4.5	Ω
Line resistance at steady state	5.34	Ω
Average winding temperature at steady state	73.9	°C

Table 5 Comparison of FEA and temperature rise test of PMLSM

Parameters	FEA	Test	Deviation
Winding temperature at steady state (°C)	84.7	73.9	10.8
Stator core temperature at steady state (°C)	62.3	57.1	5.2

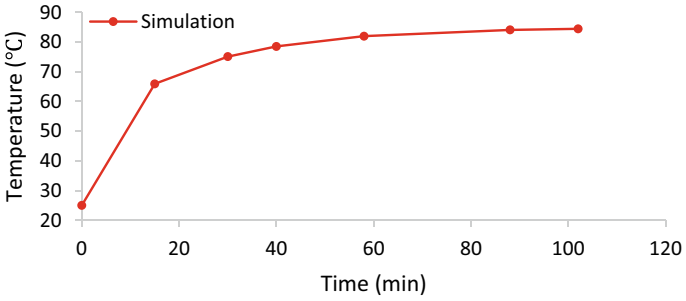

Fig. 7 PMLSM winding temperature rise curve

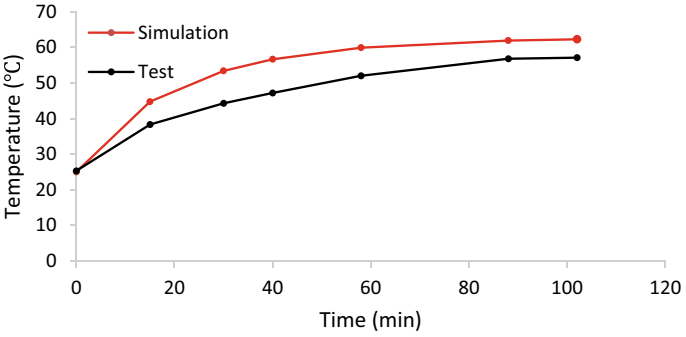

Fig. 8 PMLSM stator core temperature rise curve

of the measurement: the simulation winding temperature is the real-time value at each place of the winding, while the measured winding temperature is the average value [9]. In addition, the measured temperature of the stator core is on the outer surface, which is lower than the true temperature of the core. In the simulation, the heat transfer coefficient calculation also has deviations [10]. In summary, the finite element simulation results higher than the measured temperature, is caused by the existence of measurement errors, and is acceptable.

5 Conclusion

In this paper, based on the PMLSM test platform, a three-dimensional temperature field FEA model of the linear motor is established, and the analysis results are consistent with the experiment results, which verifies the feasibility of the 3D FEA method to analyse the temperature rise of linear motors. Moreover, through the three-dimensional finite element analysis method, the temperature of each part of the linear motor can be more accurately and comprehensively understood, which will help to achieve a more reasonable design.

References

1. Lu Q, Zhang X, et al (2015) Modeling and investigation of thermal characteristics of a water-cooled permanent-magnet linear motor. IEEE Trans Ind Appl:2086–2096
2. Tang Y (2014) Magnetic field analysis and research on electromagnetic force of permanent magnet linear synchronous motor for precision motion platform. Harbin Institute of Technology
3. Li Y, Yan J, Xia J (2015) Temperature field analysis of line-start asynchronous permanent magnet motor based on fluent. J Electr Eng:15–21
4. Amoros JG, Andrada P, Blanque B (2010) An analytical approach to the thermal design of a double-sided linear switched reluctance motor. In: International conference on electrical machines
5. Mu X (2012) Research on the thermal characteristic of a flat permanent-magnet liner synchronous motor feeding system. Zhejiang University
6. Tai Y, Liu Z (2010) Analysis on three-dimensional transient temperature field of induction motor. Proc CSEE:114–120
7. Zhang X, Ren Z, Mei F (2007) Heat transfer, 5th edn. China Construction Industry Press, Beijing
8. Kreith F, et al (2011) Principles of heart transfer.7th edn. Cengage Learning
9. Zhang X (2014) Research on thermal behavior and thrust force of water-cooled permanent magnet liner motor. Zhejiang University
10. Wang H (2014) Fluid dynamics as I understand it. Defense Industry Press, Beijing